Resolving the structure of warm dense materials

Luke B. Fletcher

SLAC National Accelerator Laboratory

June 30th, 2015 – Frontiers of Plasma Science Town Meeting

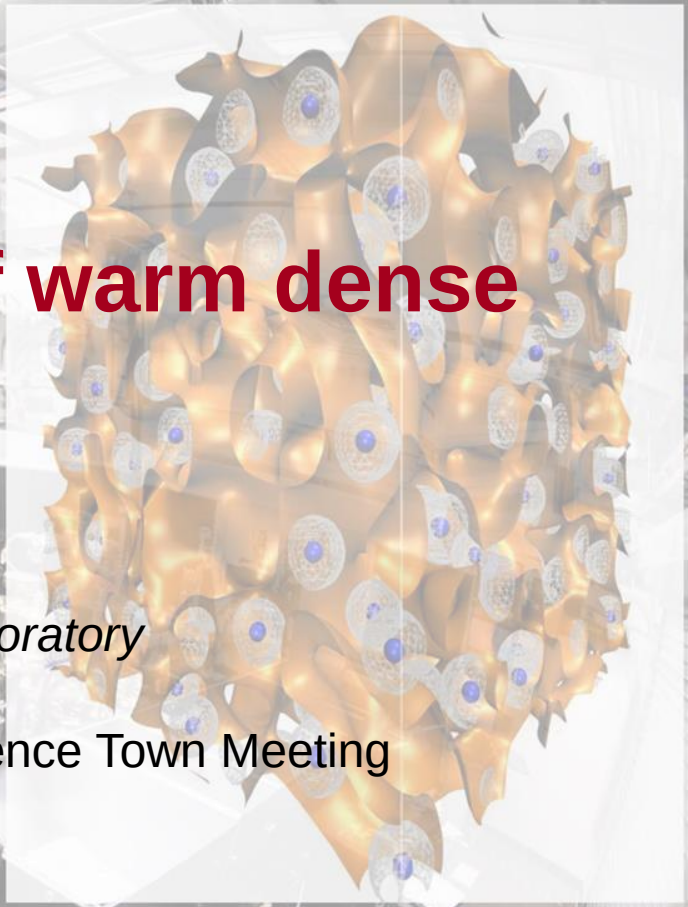

WDM physics is of considerable practical importance and it can be studied using the MEC end station of the LCLS

SLAC

Warm Dense Matter regime

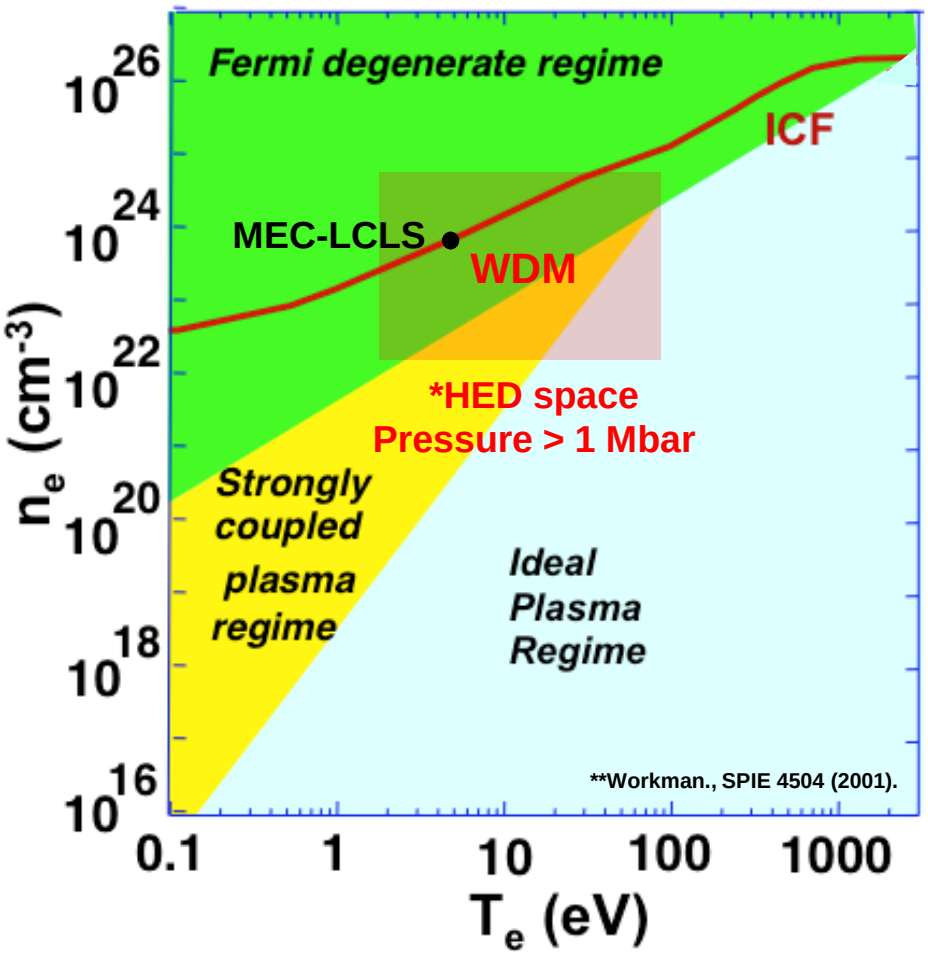

* X-rays can probe dense matter regime where optical techniques can no longer penetrate through the plasma (n_e>10^{21}/cc)

Astrophysical objects

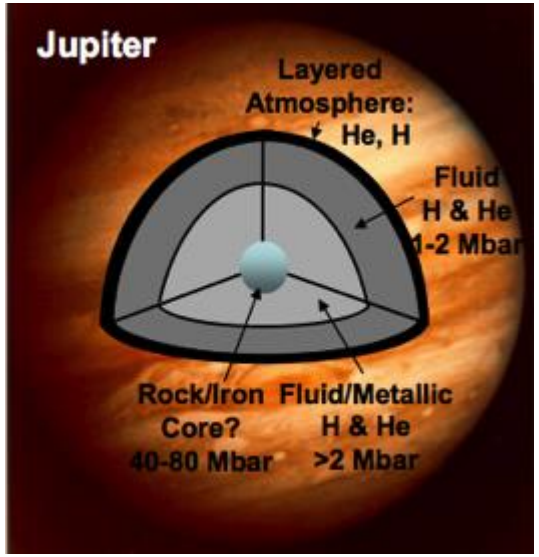

Inertial Confinement Fusion

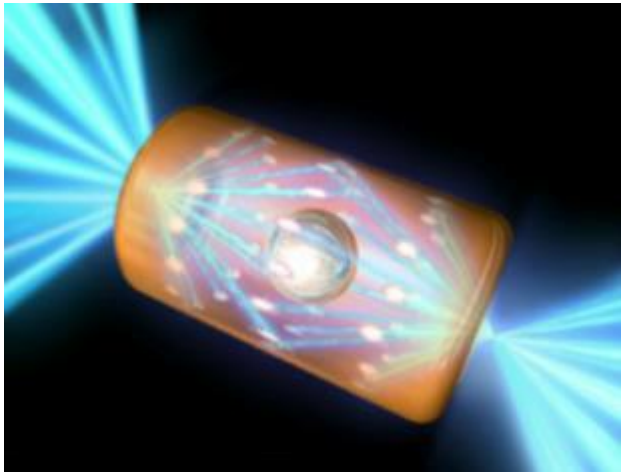

We typically do not encounter high pressure conditions

Comfortable pressure:

(Atmosphere → P = 1 bar)

Uncomfortable pressure:

(1 Large African Elephant*)

***7 tons per square inch**

We typically do not encounter high pressure conditions

Bottom of the ocean
(P = 1,000 bar = 1 kbar)

5 Large African Elephants

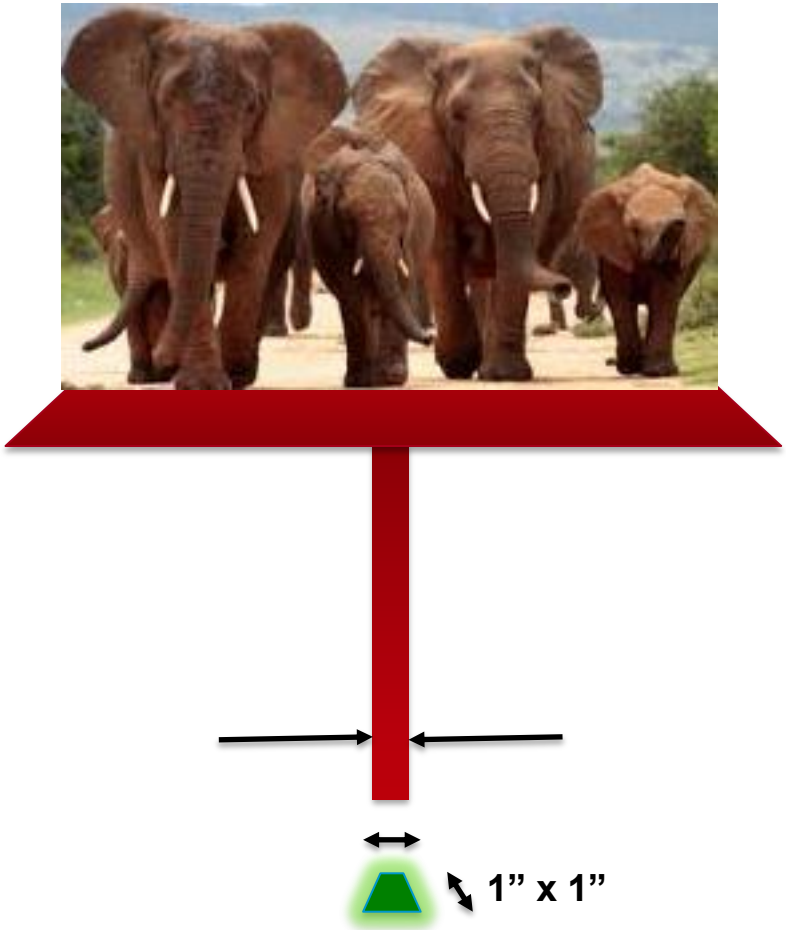

We typically do not encounter high pressure conditions

MEC reaches Jupiter interior

(P = 5,000,000 bar = 5 Mbar*)

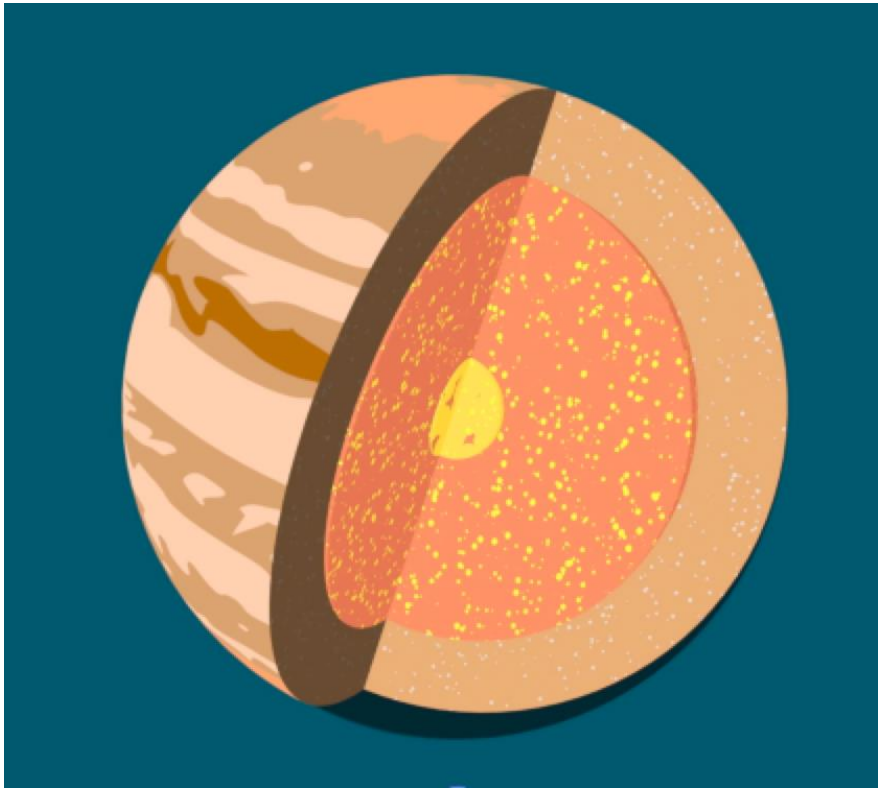

5,000 Large African Elephants

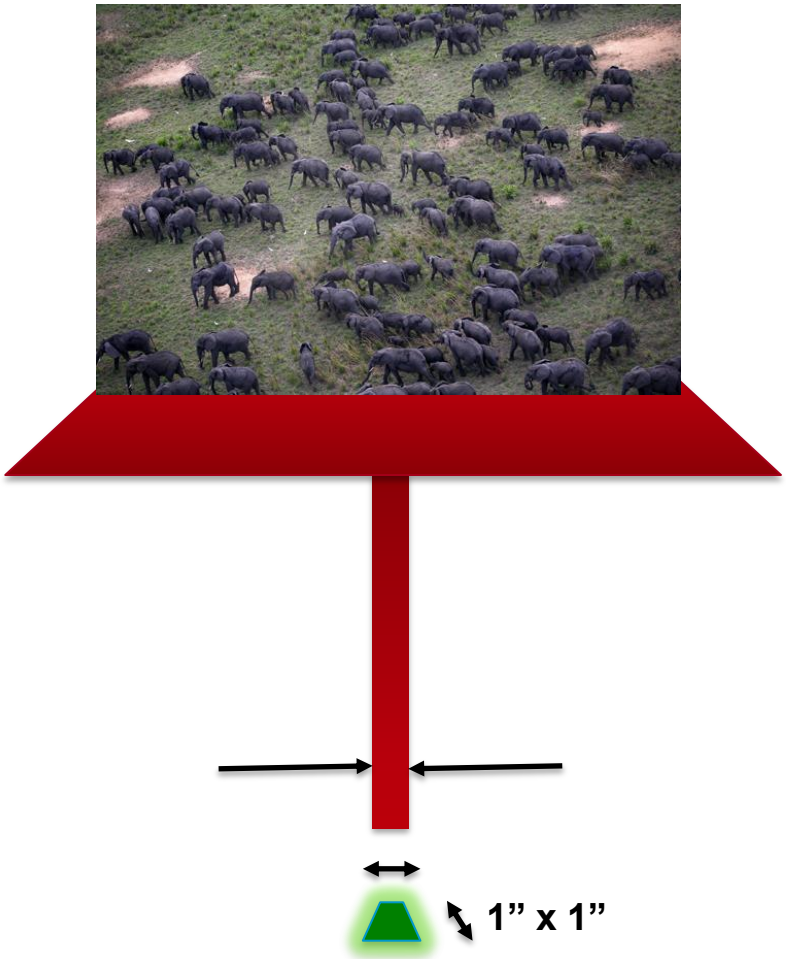

*** ~2x the pressure in the center of Earth**

Linac Coherent Light Source at *SLAC*

X-FEL based on last 1-km of existing 3-km linac

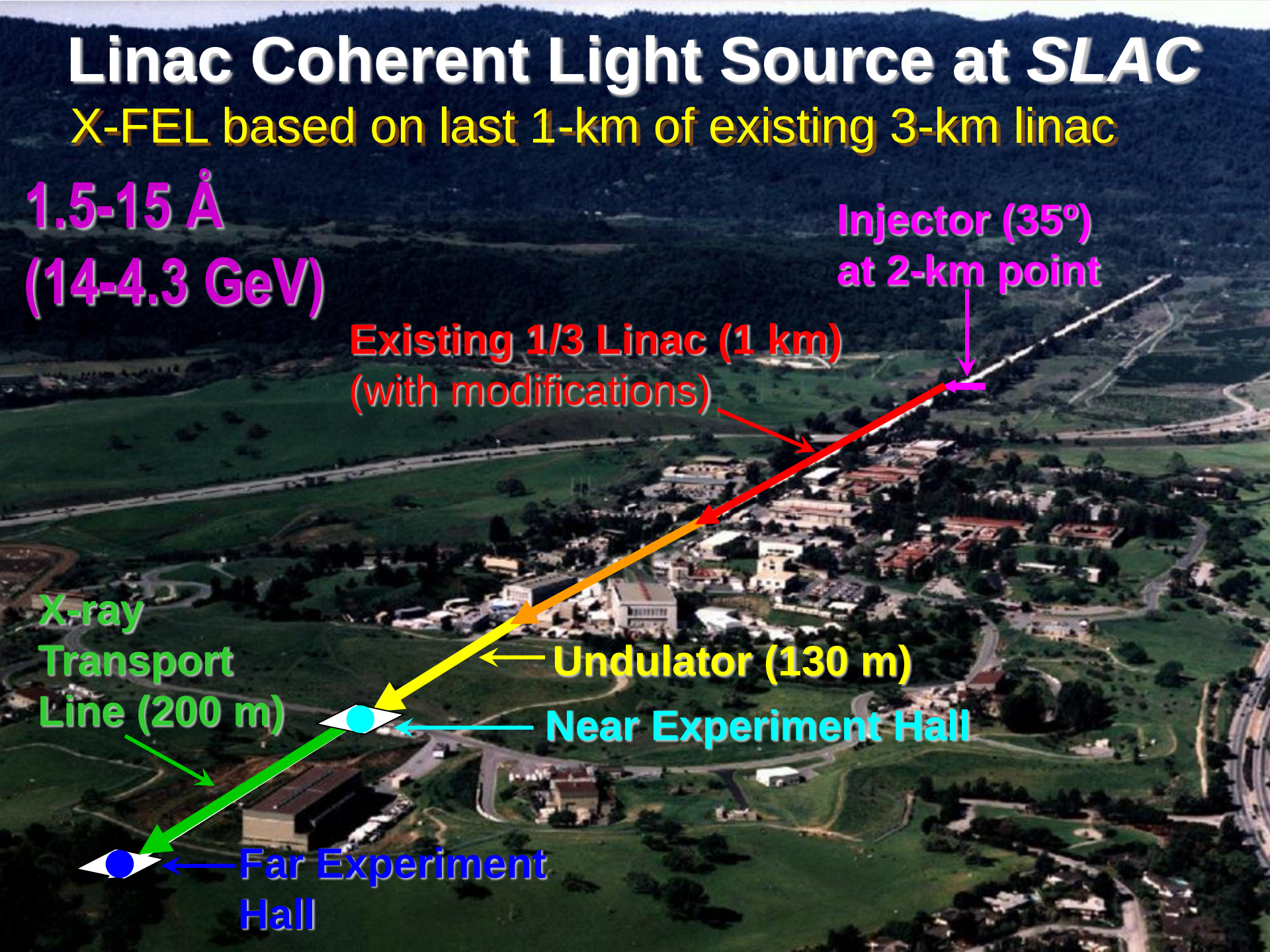

LCLS Matter in Extreme Conditions (MEC) instrument

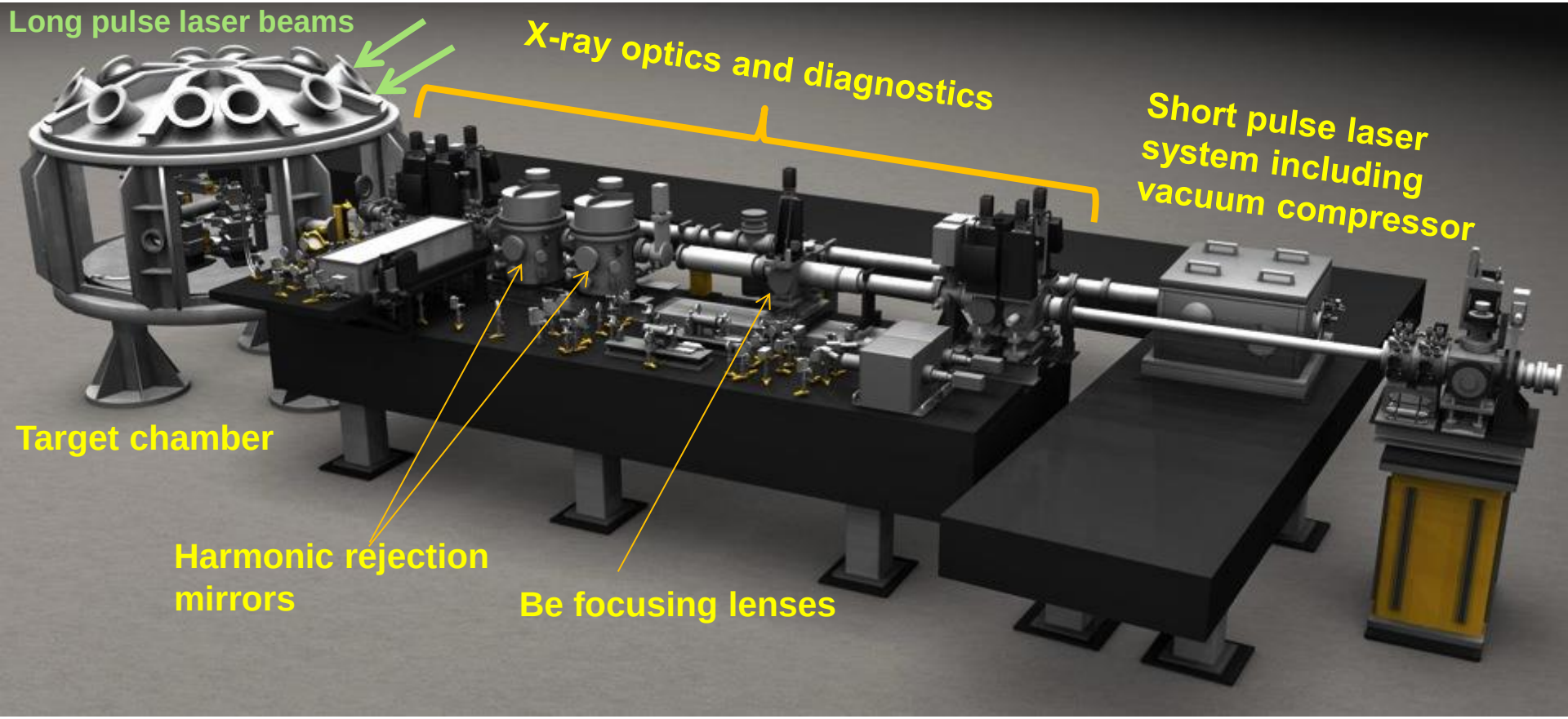

FEL current performance	
Photon energy range	480 to 10,000 eV
FEL pulse length	5 - 500 fs
FEL pulse energy	up to 4 mJ

	Long pulse laser	Short pulse laser
Wavelength	527 nm	800 nm
Pulse width	2-200 ns	40 fs
Repetition rate	1 shot per 10 minute	5 Hz
Pulse energy	2 x 15 Joules	1 Joule

We scatter x-rays from matter to understand its nature

Free particles

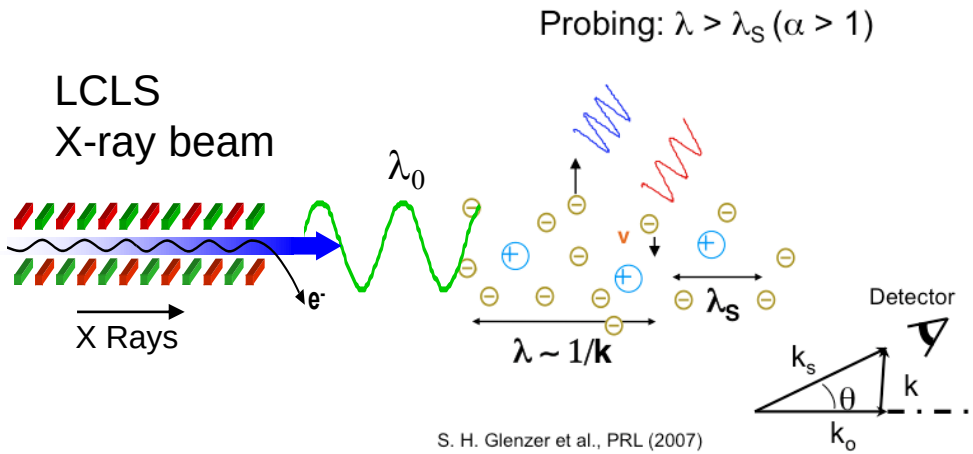

S. H. Glenzer et al., PRL (2007)

Solid with regular lattice planes

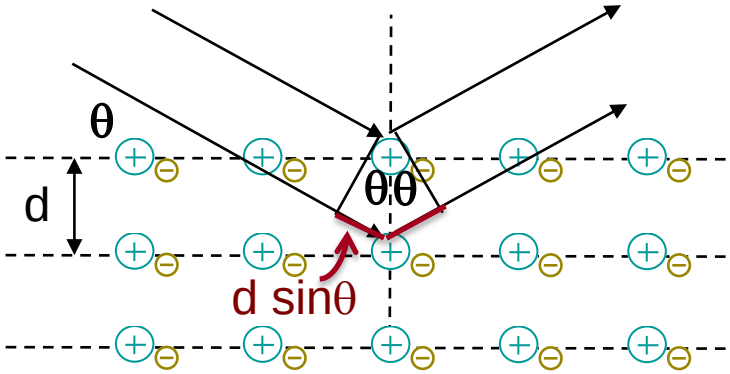

Collective scattering

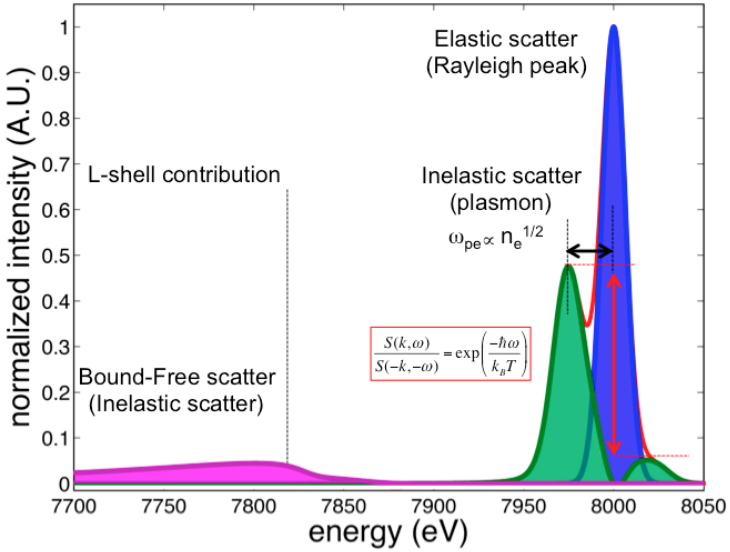

Constructive interference (Debye-Scherrer rings)

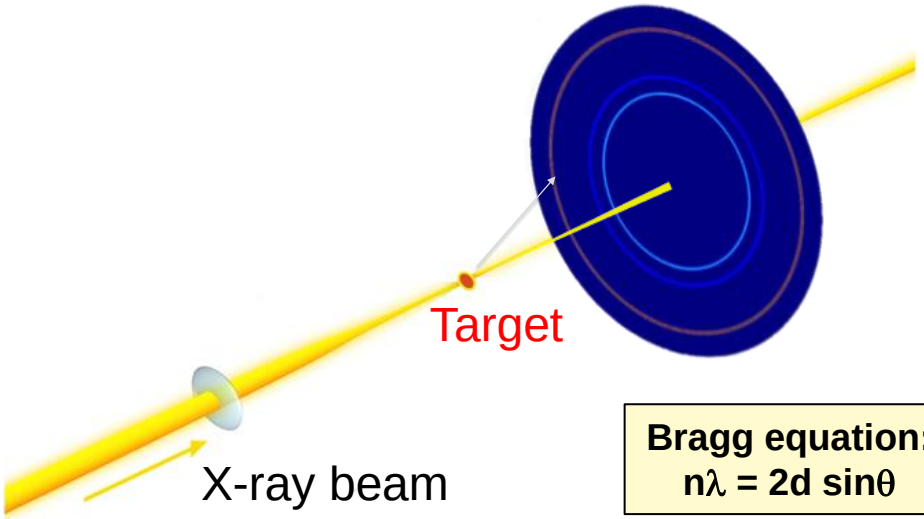

Bragg equation:
$n\lambda = 2d \sin\theta$

We scatter x-rays from matter to understand its nature

Free particles

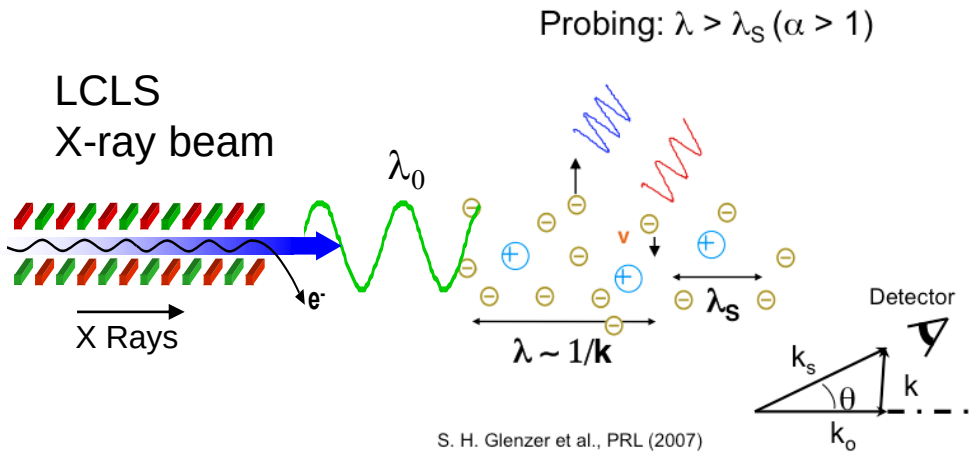

Warm Dense Matter (fluid-like)

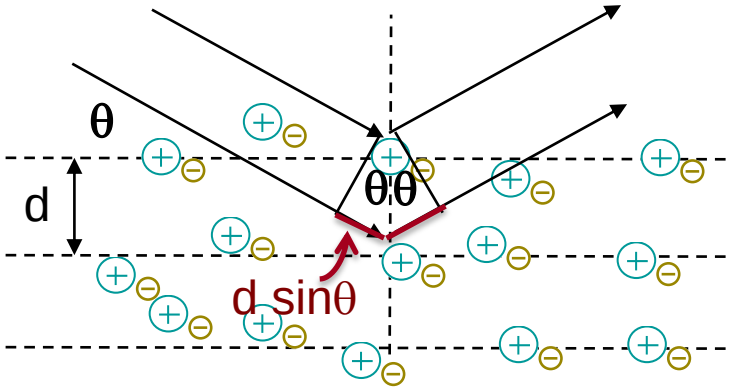

Collective scattering

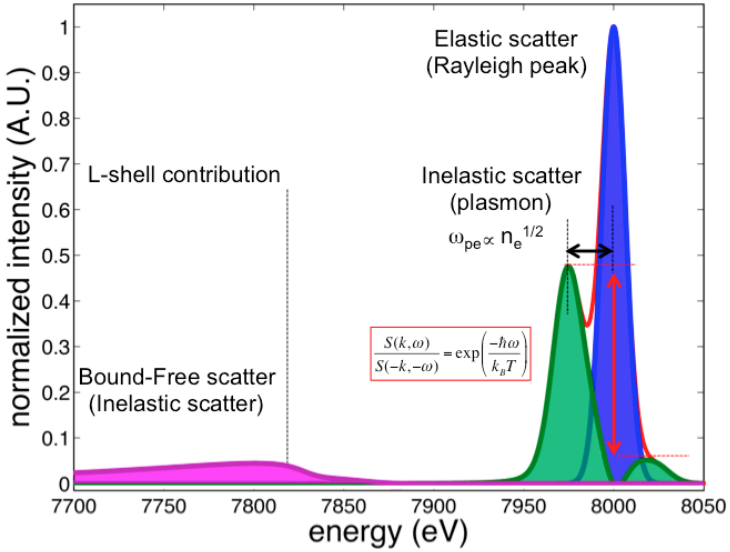

Broad scattering (result of ion motion)

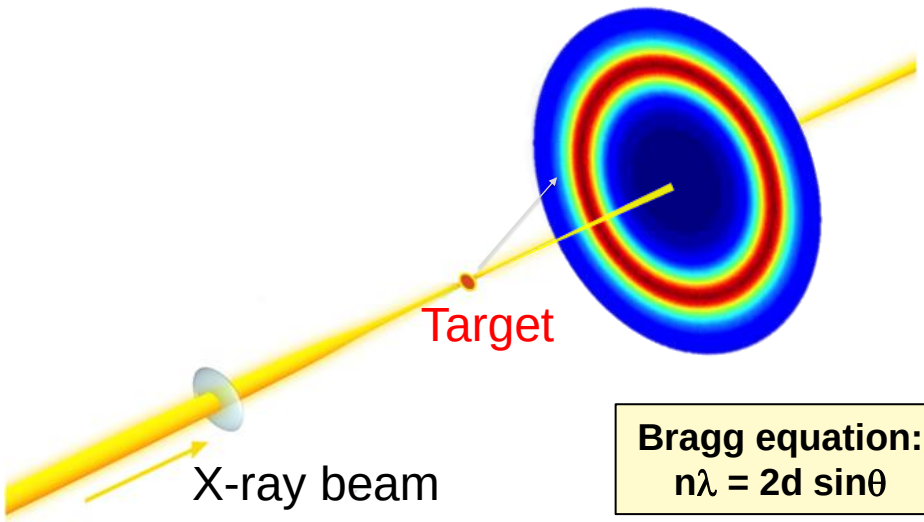

Bragg equation:
$n\lambda = 2d \sin\theta$

Models for the ionic structure in warm dense aluminum predict oscillations in the $S_{ii}(k)$

The total scattered intensity

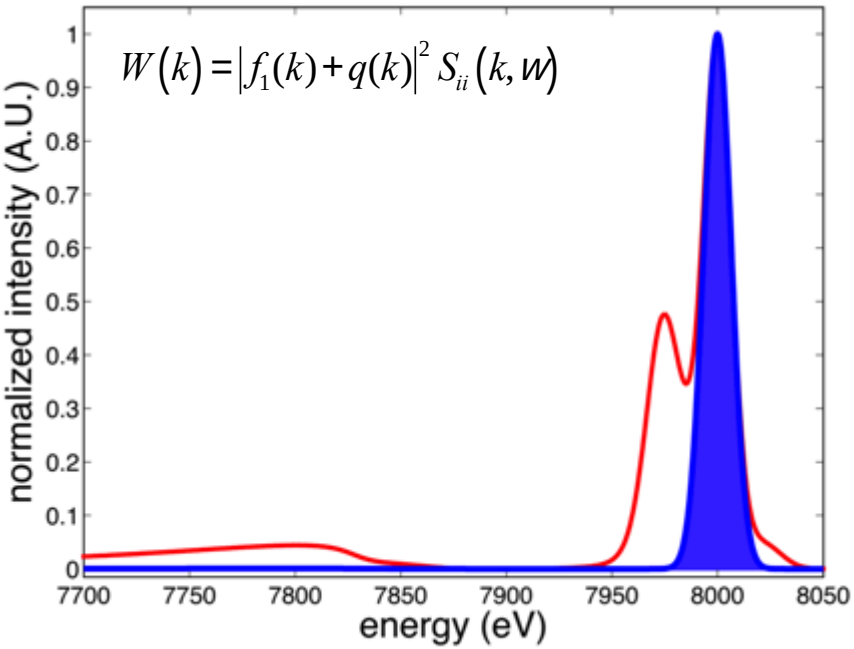

Ion-ion correlation peak

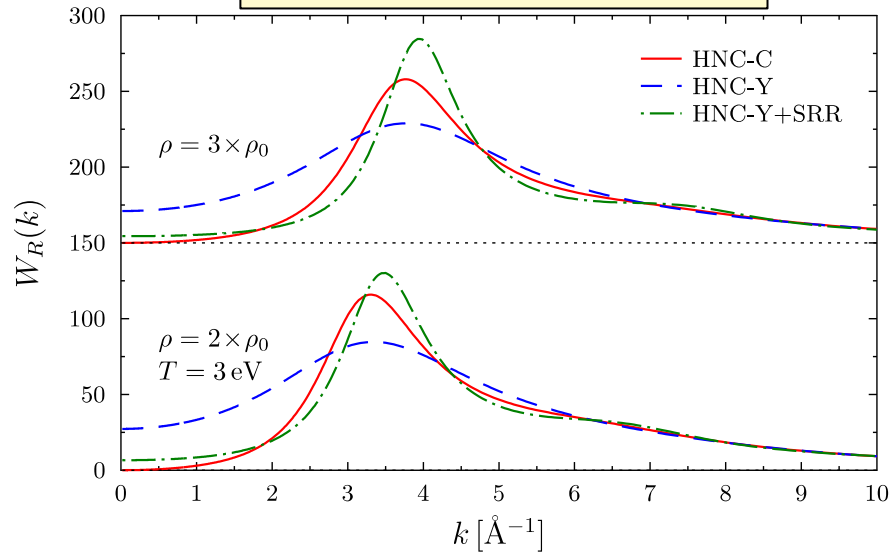

Pseudopotentials account for polarisable free electron background & bound core electrons

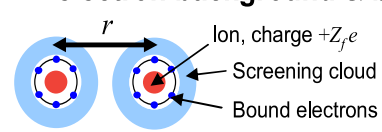

$$\beta V_{ii}(r) = \frac{Z_f^2 e^2}{r k_B T} e^{-\kappa_e r} + \frac{\sigma^4}{r^4}$$

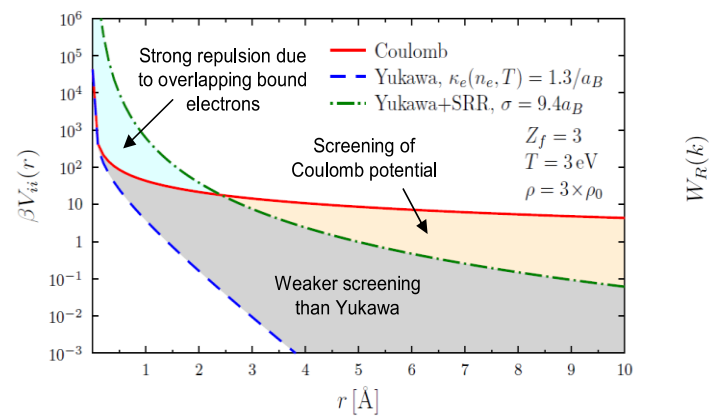

- The predicted static ion-ion structure factor for Al shows strong oscillations with a well pronounced peak that shifts to higher k as a function of compression
- Angularly resolved elastic scattering can be used to characterize the electron density as well as understand the nature of screening

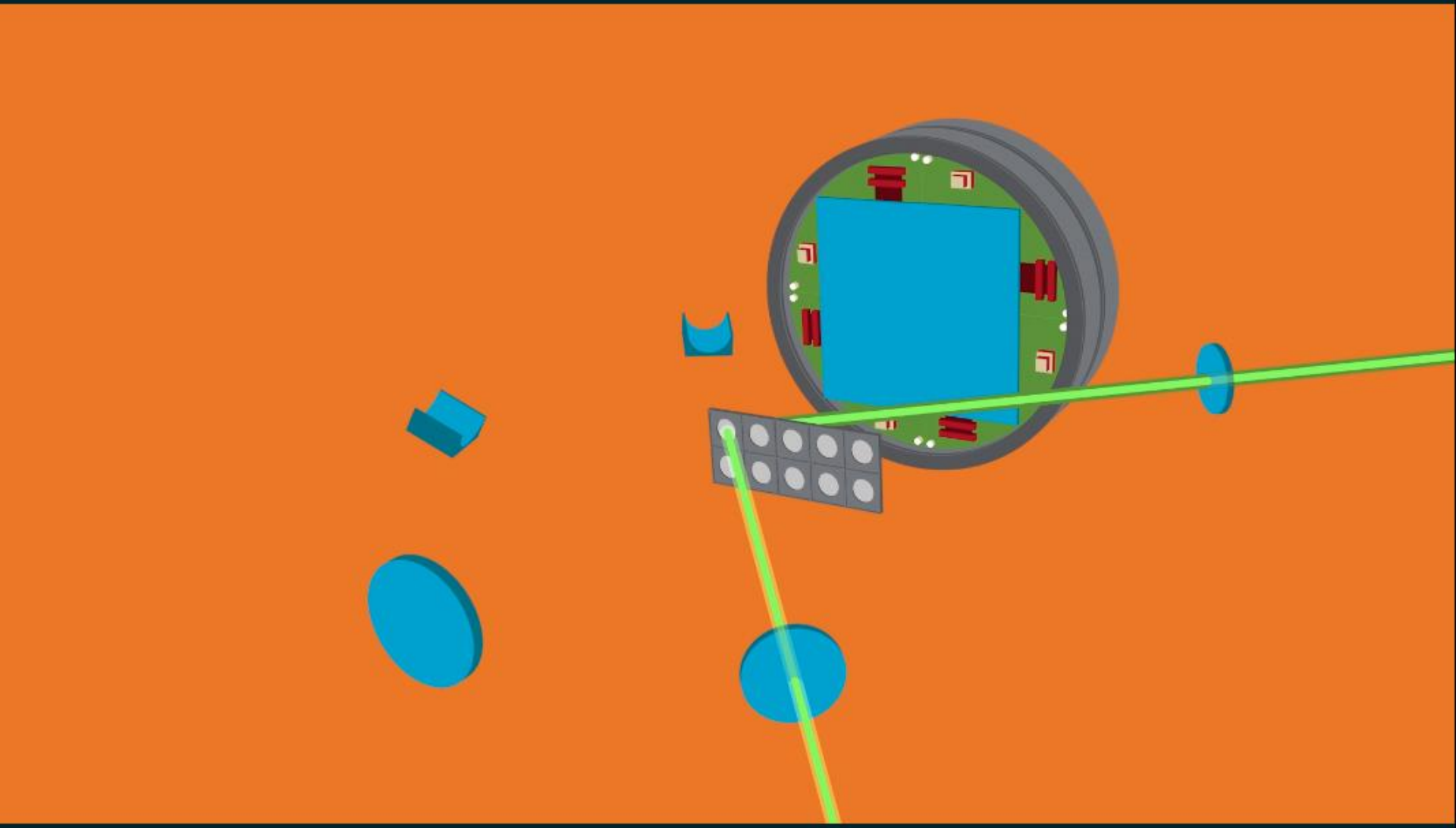

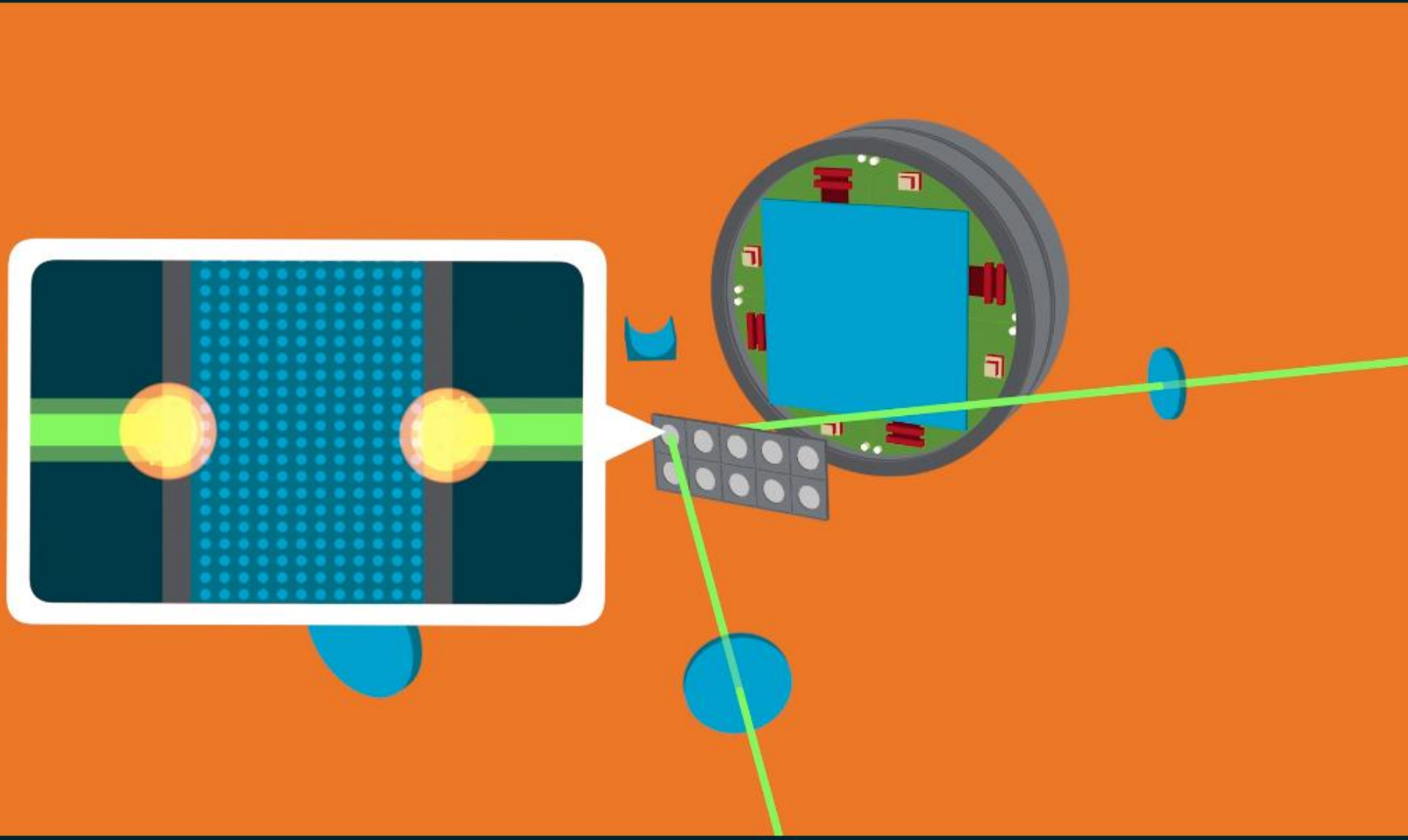

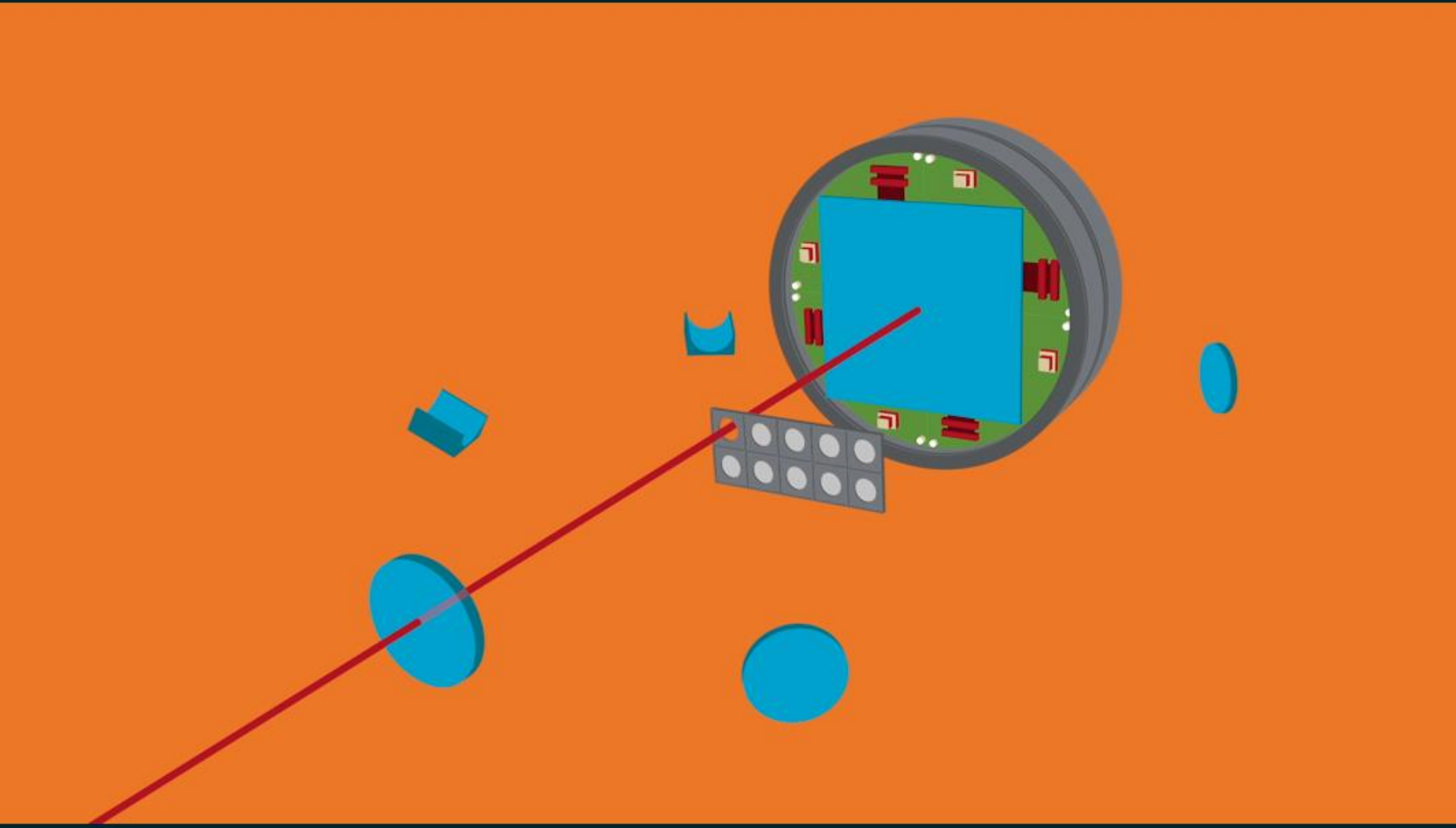

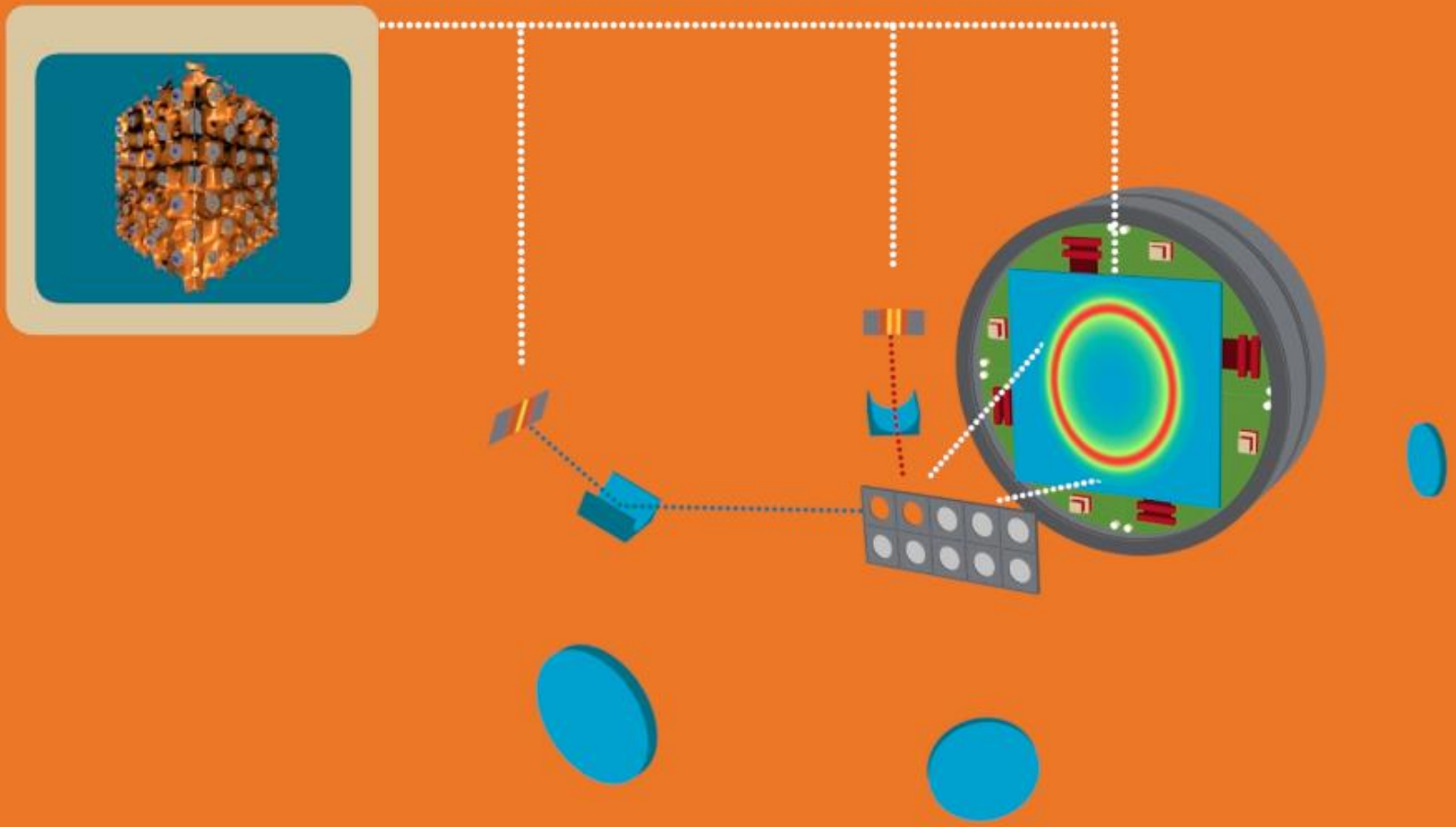

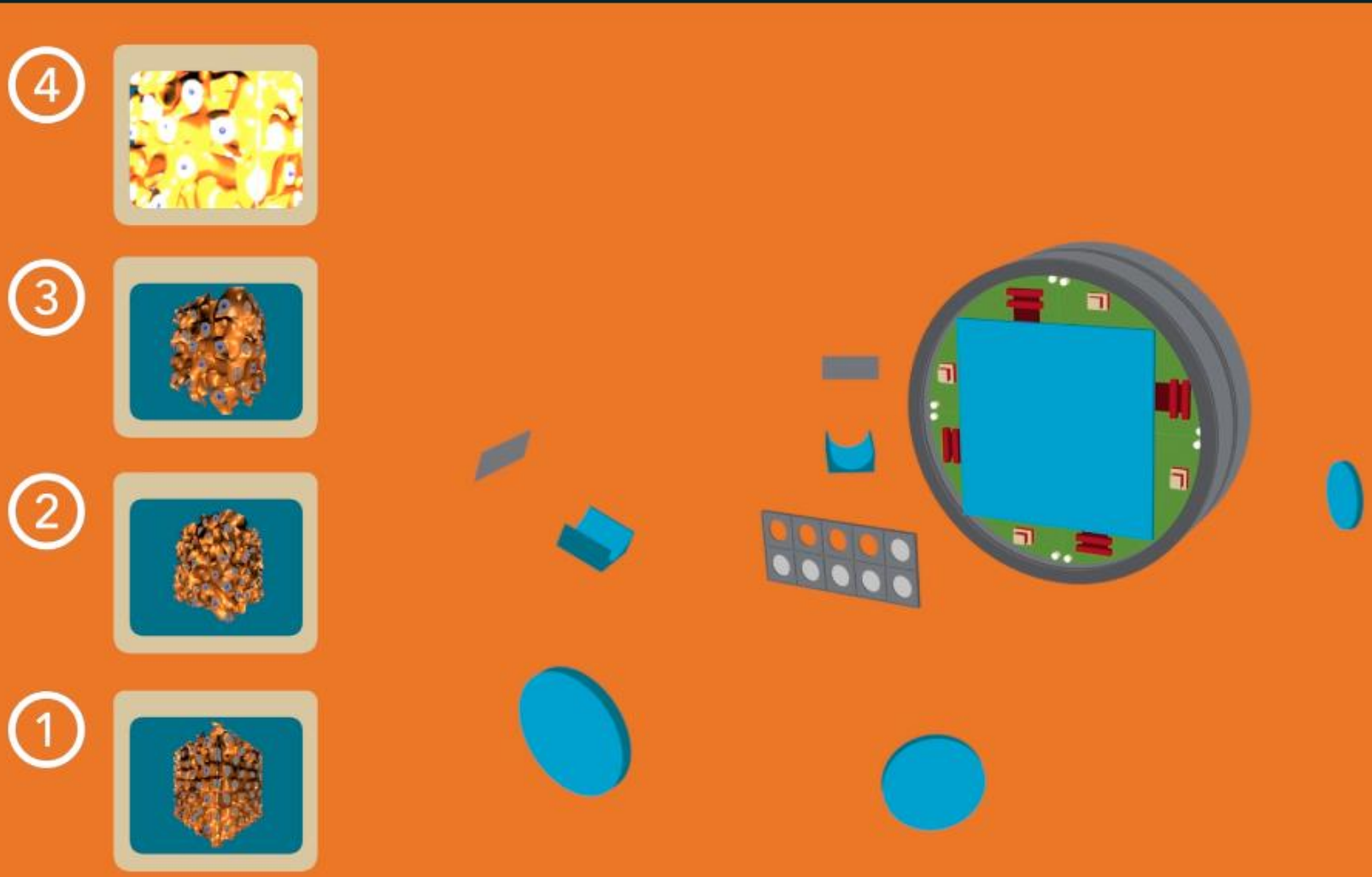
4
3
2
1

Angularly resolved elastic scattering can be used to understand the structure and properties of warm dense matter

SLAC

Structure of aluminum modeled by DFTMD

Initial State

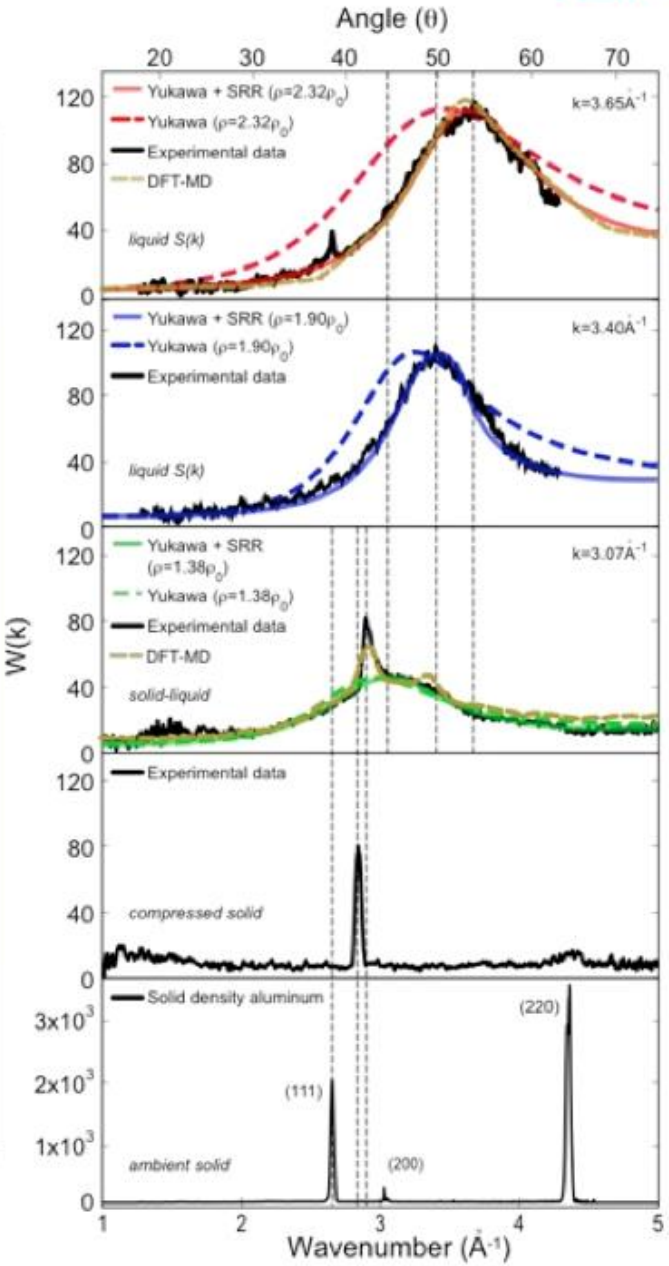

L. Fletcher *et al. Nature Photonics* **9**, 274 – 279 (2015)

Angularly resolved elastic scattering can be used to understand the structure and properties of warm dense matter

SLAC

Structure of aluminum modeled by DFTMD

Initial State

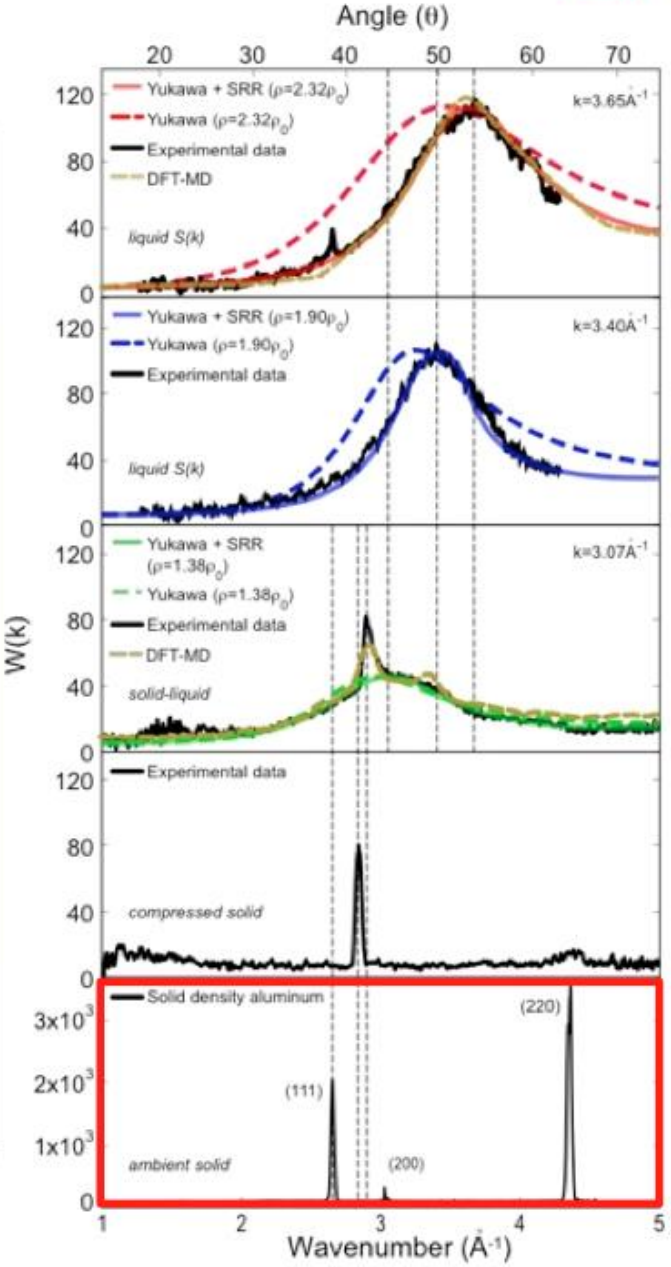

L. Fletcher *et al. Nature Photonics* **9**, 274 – 279 (2015)

Angularly resolved elastic scattering can be used to understand the structure and properties of warm dense matter

SLAC

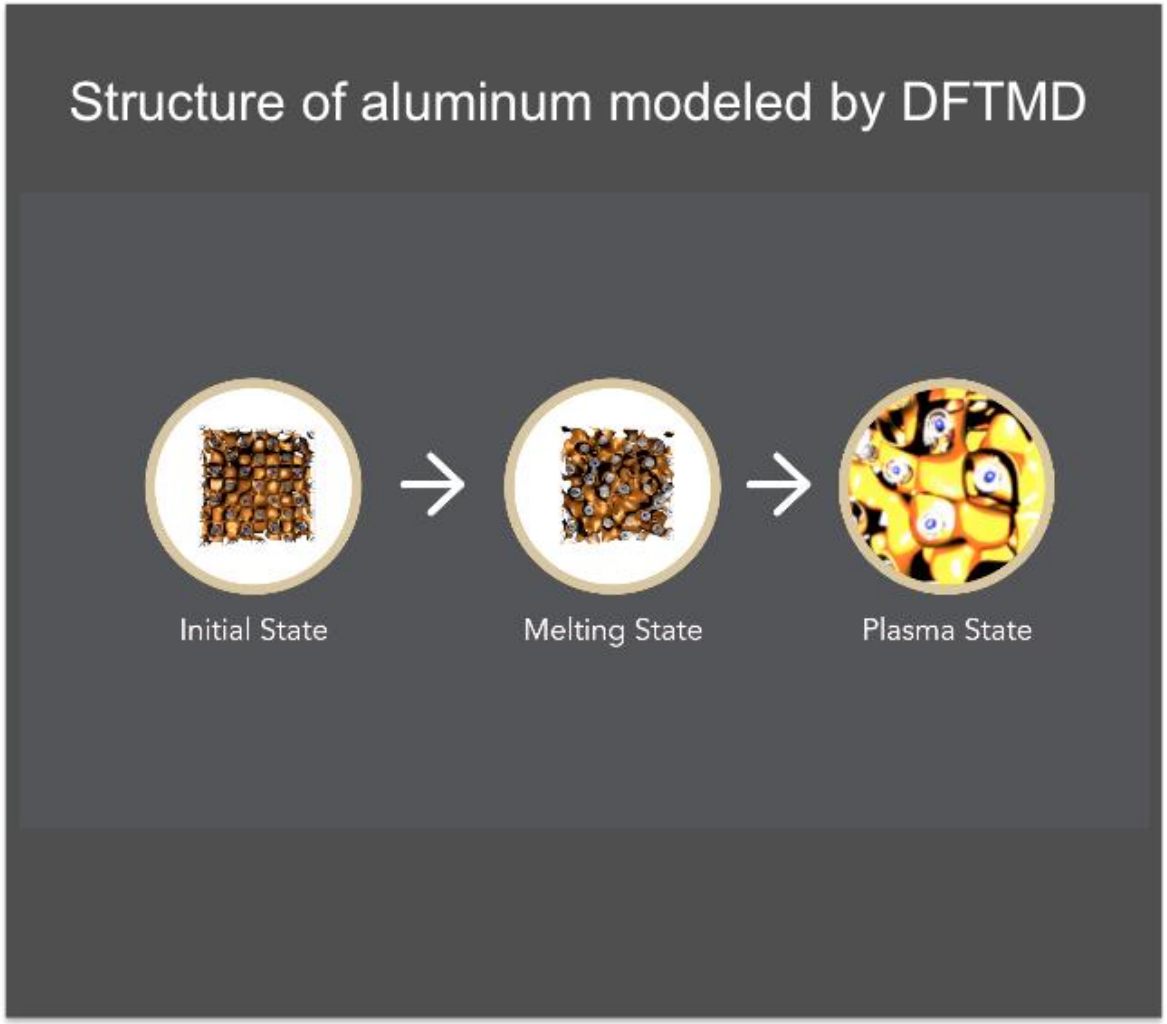

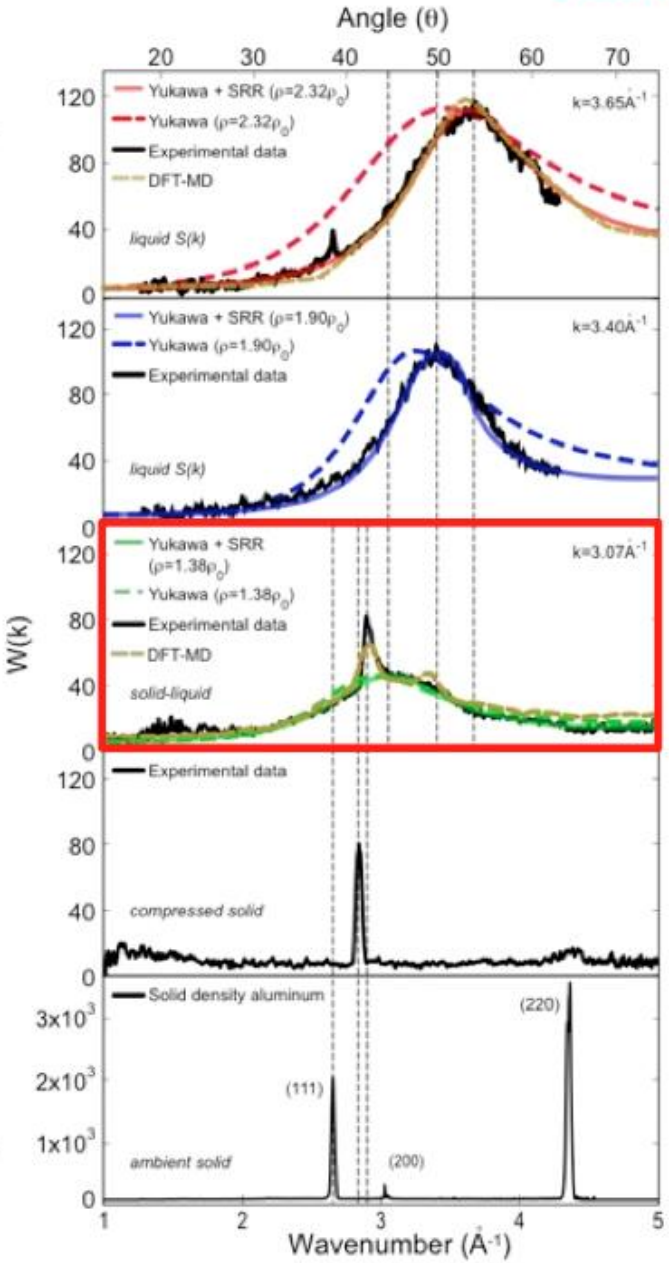

L. Fletcher *et al. Nature Photonics* **9**, 274 – 279 (2015)

Angularly resolved elastic scattering can be used to understand the structure and properties of warm dense matter

SLAC

Structure of aluminum modeled by DFTMD

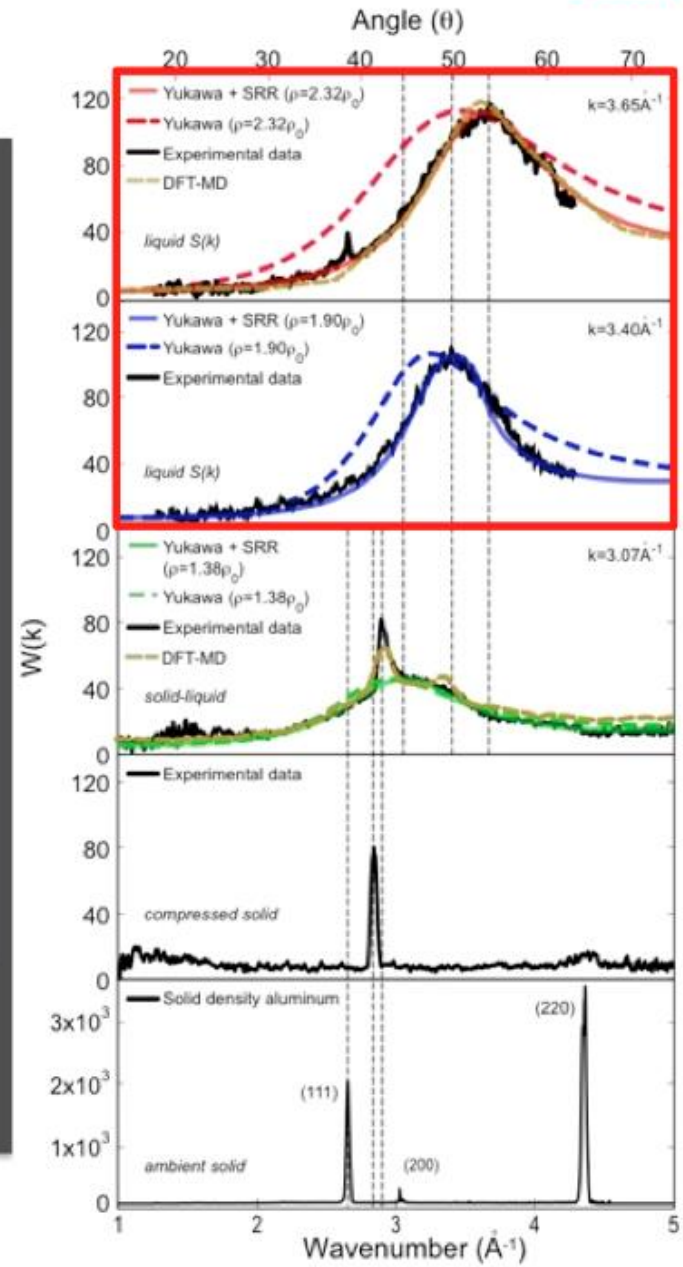

L. Fletcher *et al. Nature Photonics* **9**, 274 – 279 (2015)

Angularly resolved elastic scattering can be used to understand the structure and properties of warm dense matter

SLAC

Structure of aluminum modeled by DFTMD

Warm Dense Matter

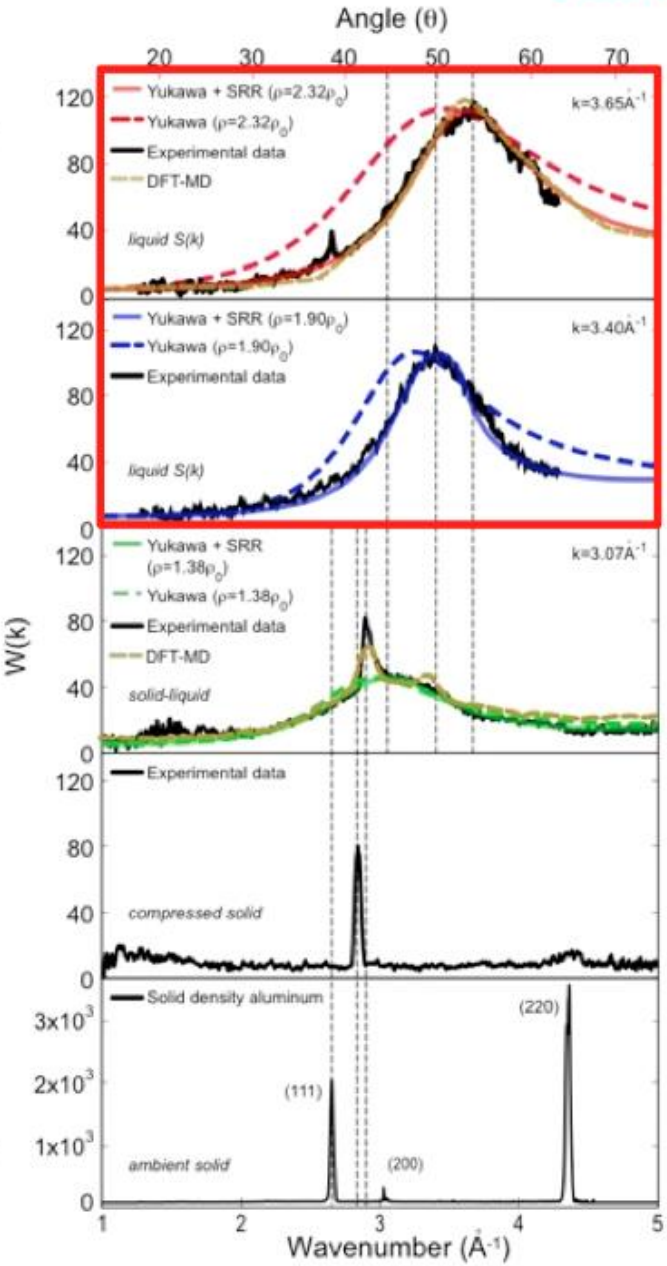

L. Fletcher *et al. Nature Photonics* **9**, 274 – 279 (2015)

LCLS data is consistent with previous Omega campaigns

Measured ion-ion correlation peak (2 years)

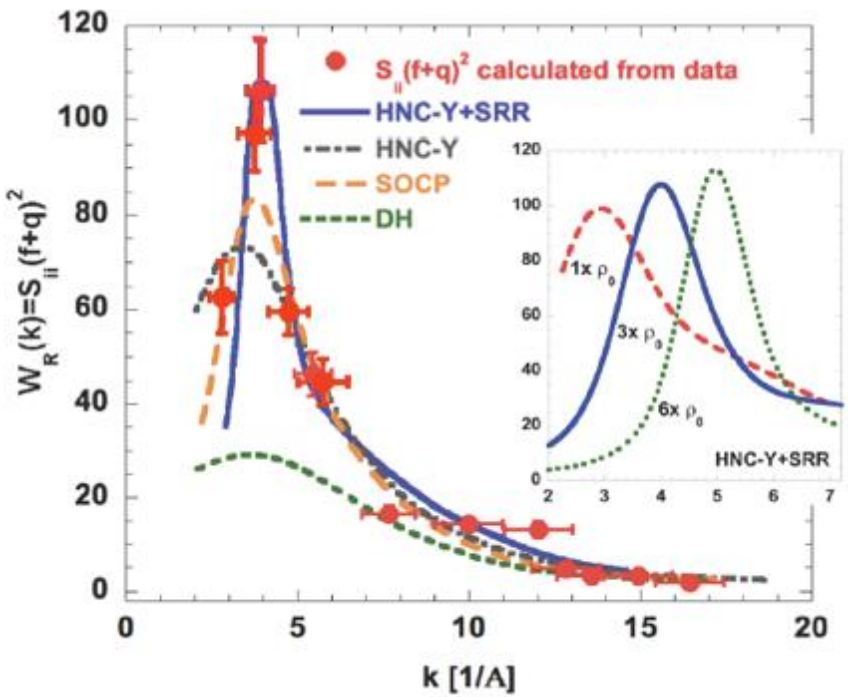

The shift and change in peak intensity of the correlation peak for 1.9x and 2.3x compressed aluminum, modeled using HNC-Y+SRR, can serve as a dynamic density diagnostic

Ion-ion correlation peak (single shot – 7 min)

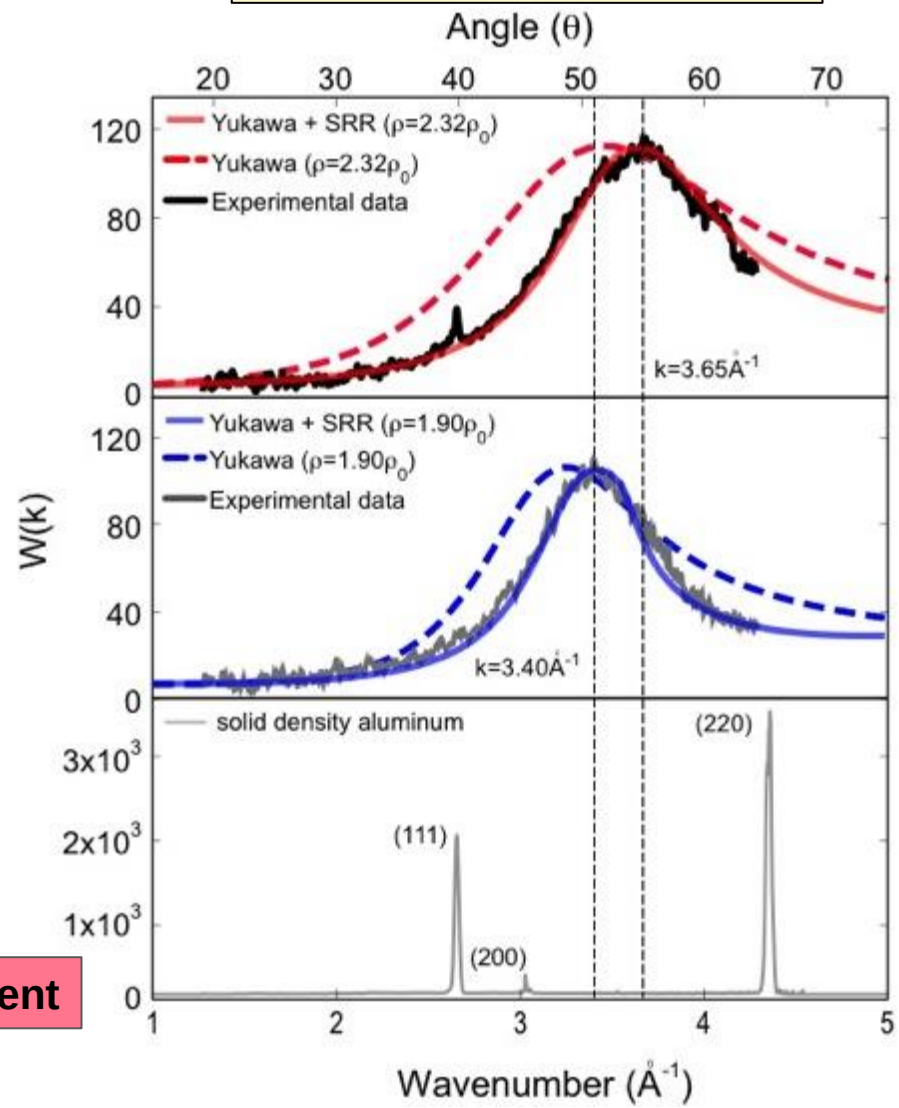

Continuous wavenumber resolved measurement

T. Ma *et al.*, *PRL 110, 065001 (2013)*

The internal energy per particle (and consequently the pressure) depends on S(k)

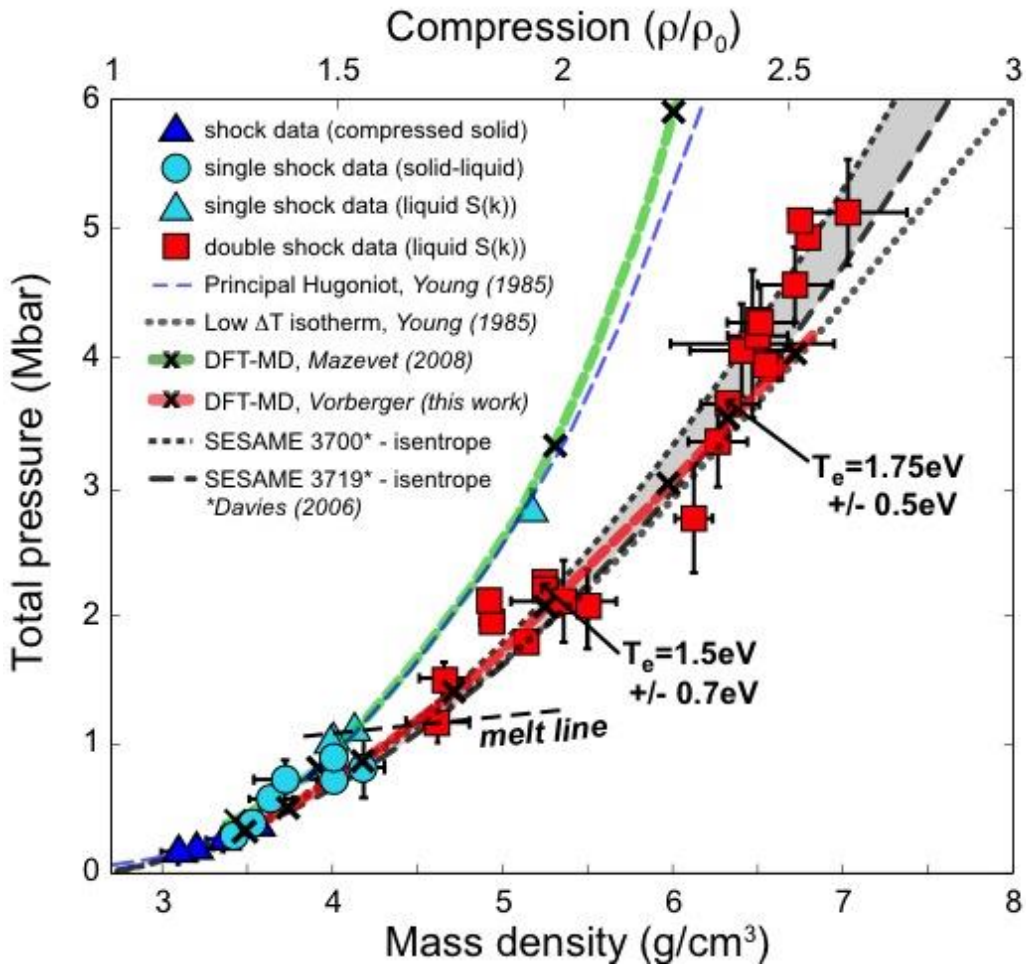

Can account for as much as 2 Mbar

Total pressure - $P(n_e, T_e, S(k))$

$$P_{TOT} = P_i + P_e$$

Ion pressure

$$P_i = p^x + P_G$$

Excess ion pressure [1]

$$p^x = \frac{n_i U^{(0)}}{3N} - \frac{n_i (Ze)^2}{12p^2} \int_0^\infty S(k) \frac{k_e^4}{(k^2 + k_e^2)^2} dk$$

Ideal gas pressure

$$P_G = n_i k_B T_i$$

Electron pressure

$$P_e = P_F + P_{\deg} + P_C + P_{xc}$$

Fermi pressure [2]

$$P_F = \frac{h^2}{20 m_e} \left(\frac{3}{p}\right)^{2/3} n_e^{5/3}$$

Quantum electron degeneracy pressure [3]

$$P_{\deg} = \frac{p m_e^4 c^5}{3h^3} \left[R(2R^2 - 3)\sqrt{1 + R^2} + 3\sinh^{-1} R \right] \quad R = \frac{P_F}{m_e c}$$

Coulomb negative pressure [3]

$$P_C = -\frac{8p^3 m_e^4 c^5}{h^3} \left[\frac{a Z^{2/3}}{10p^2} \left(\frac{4}{9p}\right)^{1/3} R^4 \right] \quad a = \frac{e^2}{4p e_0 \hbar c}$$

Electron-exchange pressure [3]

$$P_{xc} = -\frac{2a m_e^4 c^5}{h^3} b^*$$

[1] Galam and Hansen, Phys Rev. A, 14 (1976)

[2] R. P. Drake, *High-Energy-Density Physics,* (2006)

[3] P. K. Shukla *et al*., Phys. Rev. E, 87 (2013)

200 J drive laser beam can be used to explore the electronic shell structure in high-energy-density plasmas

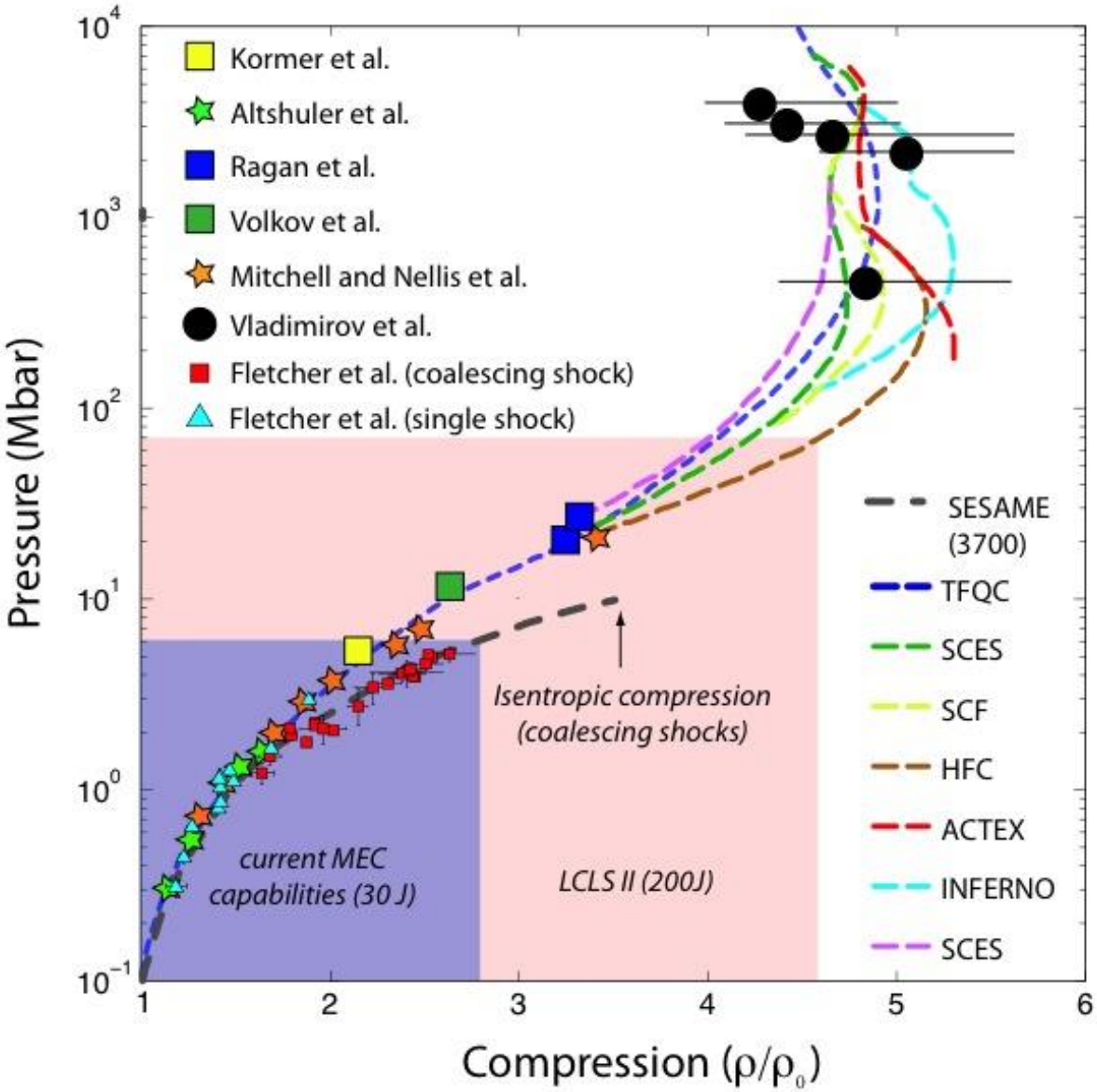

- A variety of theoretical methods, plotted for high pressure and compression, where the various models exhibit differences in predicted conditions due to k-shell ionization behavior in highly compressed aluminum
- High precision capabilities of LCLSII together with a 200J drive beam can be used as a platform to evaluate different EOS models in high-energy-density states of matter
- Current laser driver capabilities at MEC only allow for exploration of materials at conditions below 10 Mbar

Acknowledgements

T. Ma[2], A. Pak[2], T. Döppner[2], C. Fortmann[2], O. L. Landen[2], D. Turnbull[2], S. LePape[2], S. Hamel[2], D. A. Chapman[3,4], D. O. Gericke[4], T. White[5], G. Gregori[5], D. Kraus[1], B. Barbrel[1], M. Wei[7], J. Vorberger[8], M. MacDonald[9], P. Sperling[10], D. Cebulla[10], A. Ravasio[11,12], E. Gamboa[12], M. Gauthier[12], R. Mishra12, U. Zastrau[12], B. Nagler[12], H. J. Lee[12], E. Galetier[12], A. Gleason[12], S. Funk[12], S. Brown[12], Z. Chen[12,13], C. Curry[12,13], F. Fiuza[12], A. Fry[12], S. Goede[12], C. Roedel[12], P. Sperling[10,12], W. Schumaker[12], Y. Y. Tsui[12,13], F. Fiuza[12], J. Hastings[12], R.W. Falcone[1,6], and S.H. Glenzer[12]

[1]University of California, Berkeley Department of Physics
[2]Lawrence Livermore National Laboratory
[3]Centre for Fusion, Space and Astrophysics, Department of Physics,
[4]University of Warwick, UK
[5]University of Oxford Department of Physics
[6]Lawrence Berkeley National Laboratory
[7]General Atomics
[8]Max Planck Institute for the Physics of Complex Systems
[9]University of Michigan
[10]University of Rostock, GER
[11]École Polytechnique, FRA
[12]SLAC National Accelerator Laboratory
[12]University of Alberta, CA

***Prepared by LLNL under Contract DE-AC52-07NA27344 and supported by LDRD grant 11-ER-050**
***NLUF Grants: DE-FG52-07 NA28057 & DE-DE-FG52-09 NA29035**
***This work is supported by DOE Office of Basic Energy Sciences, Materials Sciences and Engineering Division, under Contract DE-AC02-76SF00515**